Morphologic and transport properties of natural organic floc

Laurel G. Larsen,[1,2] Judson W. Harvey,[2] and John P. Crimaldi[1]

[1] The morphology, entrainment, and settling of suspended aggregates ("floc") significantly impact fluxes of organic carbon, nutrients, and contaminants in aquatic environments. However, transport properties of highly organic floc remain poorly understood. In this study detrital floc was collected in the Florida Everglades from two sites with different abundances of periphyton for use in a settling column and in racetrack flume entrainment experiments. Although Everglades flocs are similar to other organic aggregates in terms of morphology and settling rates, they tend to be larger and more porous than typical mineral flocs because of biostabilization processes and relatively low prevailing shear stresses typical of wetlands. Flume experiments documented that Everglades floc was entrained at a low bed shear stress of 1.0×10^{-2} Pa, which is considerably smaller than the typical entrainment threshold of mineral floc. Because of similarities between Everglades floc and other organic floc populations, floc transport characteristics in the Everglades typify the behavior of floc in other organic-rich shallow-water environments. Highly organic floc is more mobile than less organic floc, but because bed shear stresses in wetlands are commonly near the entrainment threshold, wetland floc dynamics are often transport-limited rather than supply limited. Organic floc transport in these environments is therefore governed by the balance between entrainment and settling fluxes, which has implications for ecosystem metabolism, materials cycling, and even landscape evolution.

Citation: Larsen, L. G., J. W. Harvey, and J. P. Crimaldi (2009), Morphologic and transport properties of natural organic floc, *Water Resour. Res.*, *45*, W01410, doi:10.1029/2008WR006990.

1. Introduction

[2] Aggregation of sediment and organic matter is ubiquitous in lacustrine, palustrine, riverine, estuarine, and marine environments. Flocculation of material to form aggregates ("floc") can be enhanced by dissolved cations, which neutralize negative charges on the surface of constituent particles, allowing Van der Waals forces to bind aggregates [*Tsai et al.*, 1987; *Droppo and Ongley*, 1994]. Neutrally charged organic substances also promote cohesion. These extracellular polymeric substances (EPS) [e.g., *Wotton*, 2005], which consist of polysaccharides and proteins, wrap around multiple constituent particles and bind them through bipolar forces and hydrogen bonding [*Droppo and Ongley*, 1992; *Liss et al.*, 1996; *Droppo et al.*, 1997]. The resulting flocs have porous, fractal structures, with single-floc bulk densities that are variable but lower than the constant density of the primary particles (i.e., constituent material) [*Logan and Wilkinson*, 1990; *Khelifa and Hill*, 2006].

[3] Structural characteristics of floc, such as its cohesiveness and variability in porosity and shape, cause entrainment rates, size distributions, and settling velocities of floc to differ from those of primary particles [*Walling and Moorehead*, 1989; *Droppo*, 2003, 2004]. Interparticle cohesion can increase the threshold shear stress of particle entrainment [*Grant and Gust*, 1987], while variable single-floc densities over the spectrum of floc diameters complicate prediction of settling velocity using Stokes' law [*Tambo and Watanabe*, 1979; *Lick et al.*, 1992; *Khelifa and Hill*, 2006]. These physical characteristics have implications for turbidity and settling fluxes in estuaries [*Wolanski and Gibbs*, 1995], floodplains [*Nicholas and Walling*, 1996], the ocean [*Alldredge and Silver*, 1988], mangrove forests [*Wolanski*, 1995; *Furukawa et al.*, 1997], and tidal marshes [*Christiansen et al.*, 2000; *Fagherazzi et al.*, 2004; *D'Alpaos et al.*, 2007]. The high surface area to volume ratio and high organic content of primary particles that aggregate to form floc also promote preferential sorption of contaminants and nutrients onto the aggregate surface and within the porous matrix [*Ongley et al.*, 1992]. Flocs contain large, diverse populations of resident microbes [*Simon et al.*, 2002; *Battin et al.*, 2003; *Wotton*, 2007] and provide a labile source of carbon to the water column and/or the benthos, impacting heterotrophy and enhancing energy transfer both up the food chain [*Wilcox et al.*, 2005] and downstream [*Newbold et al.*, 2005].

[4] Though floc composed dominantly of organic matter (referred to hereafter as organic floc) is common to many environments, its morphologic and settling characteristics are poorly understood relative to inorganic floc dynamics [*Lick et al.*, 1992; *Sterling et al.*, 2005]. In contrast to inorganic floc, organic floc transport dynamics are affected by changes in nutrient and organic carbon availability and

---

[1]Department of Civil, Environmental, and Architectural Engineering, University of Colorado, Boulder, Colorado, USA.
[2]U.S. Geological Survey, Reston, Virginia, USA.

quality that impact resident microbial communities, phytoplankton, invertebrates, and their production of EPS [*Ward et al.*, 1990, *Ruddy et al.*, 1998, *Blanchard et al.*, 2000]. Likewise, because of different formation processes and differences in constituent materials, structural linkages within and between organic flocs are likely to differ from those of inorganic floc, resulting in differences in entrainment, settling, and transport rates.

[5] A greater understanding of the general morphologic characteristics and transport properties of organic floc is needed to improve predictions of particulate organic carbon and nutrient redistribution in natural and engineered systems. Improved predictive capabilities would in turn benefit design of wastewater treatment wetlands, assessment of the role of peatlands in carbon export or sequestration in a changing climate, or floodplain and wetland restoration. For example, in the Florida Everglades, the redistribution of organic floc by flowing water is thought to regulate the development of wetland topography that is critical to ecosystem function [*National Research Council*, 2003; *Larsen et al.*, 2007]. However, because of water management, the present-day flows (90% of which range between 0.11 cm s^{-1} and 0.50 cm s^{-1} [*Harvey et al.*, 2008]) are too slow to entrain significant quantities of floc. In this environment, restoration efforts would benefit from predictions of floc entrainment, settling, and size distributions over a range of flows.

[6] In this study we performed a series of laboratory experiments on organic floc from a floodplain wetland in the Florida Everglades to assess its morphology, settling rates, and entrainment characteristics. Our objectives were as follows.

[7] 1. To ascertain transport parameters of organic floc needed to improve models and make reasonable inferences about differential erosion and sedimentation processes in shallow and slowly flowing aquatic ecosystems with both emergent vegetation and open water areas.

[8] 2. To compare physical characteristics of Everglades floc from two different sites (section 2) with riverine, estuarine, lacustrine, and marine floc.

[9] These objectives were complementary to a companion study [*Larsen et al.*, 2009] in which aggregation dynamics and the role of biological processes in the field were assessed in order to improve prediction of floc transport in the Everglades under different flow management scenarios. Together, the two studies will provide insight into how mass and nutrient transport will change under restoration scenarios that affect flow velocities through this ecosystem and will provide a complete picture of the transport dynamics of a natural organic floc in a slowly flowing aquatic ecosystem.

[10] In the present-day Everglades, the loosely consolidated floc layer is rarely suspended but forms a relatively static layer over the peat bed. Therefore, we needed to intrusively collect floc for settling column observations and also perform flow manipulations to determine entrainment characteristics. Since the range of velocities in the Everglades is low compared to rivers, estuaries, and the continental shelf [*Harvey et al.*, 2005], and since it is difficult to accurately measure bed shear stresses in these slow flows, we performed entrainment experiments in the laboratory. A prime challenge in floc studies is that the delicate nature of

flocs precludes grab sampling without structural disruption [e.g., *Eisma et al.*, 1990; *Winterwerp and van Kesteren*, 2004]. Although field conditions required us to sample floc, we took measures to minimize sampling artifacts, such as allowing laboratory floc beds to settle and reaggregate for 24 h before experimentation and using a digital floc camera (DFC) to noninvasively observe floc characteristics during experimentation. Thus, while these experiments did not exactly replicate floc characteristics from the field, they provided close estimates that improve general knowledge of natural organic floc morphodynamics.
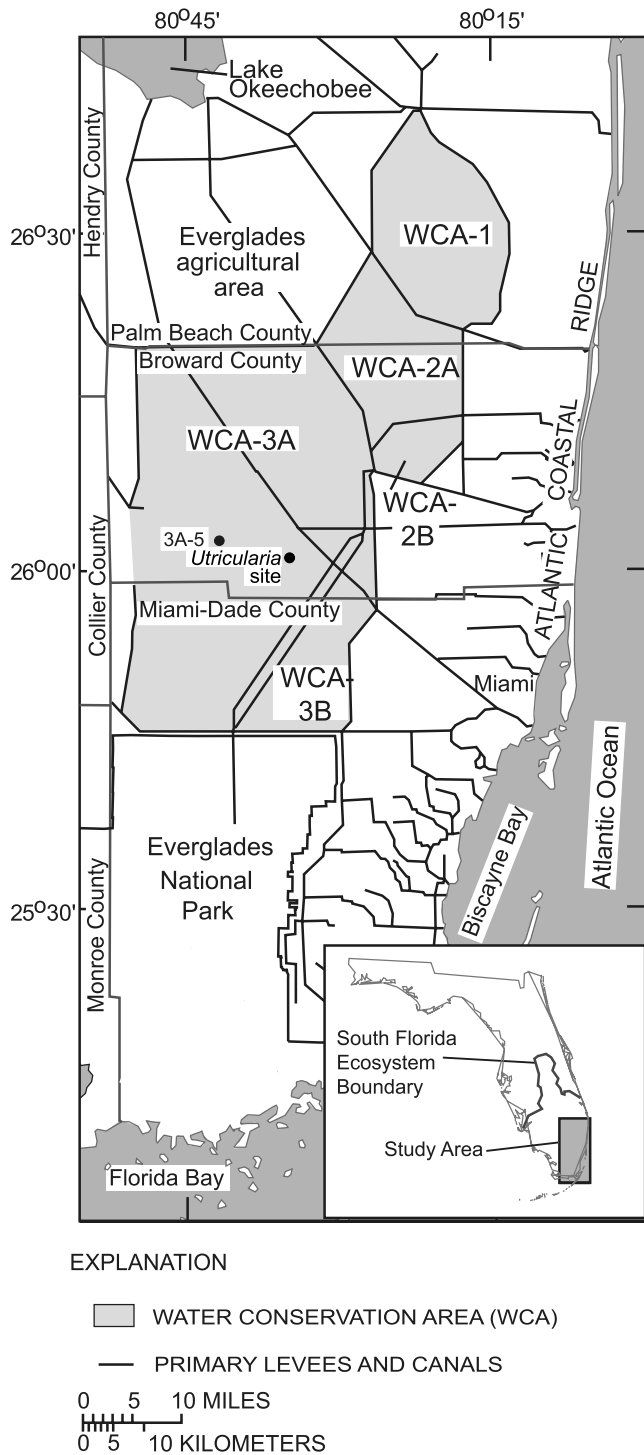
2. Site Description

[11] The Florida Everglades is a vast subtropical wetland that has experienced extensive human impact starting in the early 1900s. Impacts include agricultural discharge, loss of wetland area, altered flow depths and durations, and decreased flow velocities that are linked to compartmentalization of the landscape through the construction of levees and canals. In 2000 the Comprehensive Everglades Restoration Plan [*U.S. Army Corps of Engineers*, 1999] was authorized by U.S. Congress, providing $7.8 billion for multiple restoration objectives over its greater than 30-year lifetime.

[12] Floc samples were collected within Water Conservation Area (WCA) 3A (Figure 1), in an area of the Everglades that is thought to have hydrologic conditions most representative of predrainage conditions. One of the aggregate collection sites was site WCA-3A-5 (26°03′23.7″N, 80°42′19.2″W), a long-term research site established by the U.S. Geological Survey for the purpose of investigating flow and transport dynamics in the Everglades. At the time of collection in November 2006, the water depth was 33.5 cm. Floc at site WCA-3A-5 was not abundant at the time because of the passage of Hurricane Wilma in October 2005, followed by a complete drydown in May–July 2006, in which the water table dropped beneath the surface of the peat and the floc layer was incorporated into the peat and/or mineralized. Hurricane Wilma also eliminated the highly productive floating mats of *Utricularia* (bladderwort) and periphyton. Unlike site WCA-3A-5, the second site in WCA-3A (the "*Utricularia* site," 26° 01′ 17.9″ N, 80° 34′ 45.5″ W), maintained surface water during the summer of 2006 and had abundant floc, periphyton, and *Utricularia* at the time of sampling in November 2006. Since the *Utricularia* site was more representative of typical conditions in the historic Everglades, we used this population of floc in the laboratory flume experiment.

3. Methods

3.1. Floc Collection for Laboratory Experiments

[13] In the field the loosely consolidated layer of floc (0–12 cm thick) rests atop 75–100 cm of more highly compacted peat (mean bulk density of 0.28 ± 0.26 g cm^{-3}) [*Stober et al.*, 1998]. Using a wet/dry shop vacuum without a filter, we transferred flocculated surface sediment from 1 to 10 cm above the peat to the 7.6 L vacuum receptacle. After 5 min, the water above the settled aggregates cleared, and we concentrated the sediment/water solution by pumping off the excess water at a rate of about 200 mL min^{-1}. Just before the point of visible resuspension of particles, we

Figure 1. Locations of the Water Conservation Area (WCA)-3A-5 and *Utricularia* site floc sampling locations in the central Everglades.

ceased pumping, typically achieving a concentration factor of 2:1, and transferred the concentrated aggregates to 19-L carboys. The sediment/water mixture was shipped on ice to the laboratory, refrigerated upon arrival, and used within 1.5 weeks of collection. To create a more natural substratum for floc experiments in the laboratory flume, we also collected material from the upper 5 cm of the peat layer using a trowel. The peat was stored in plastic containers on ice prior to use.
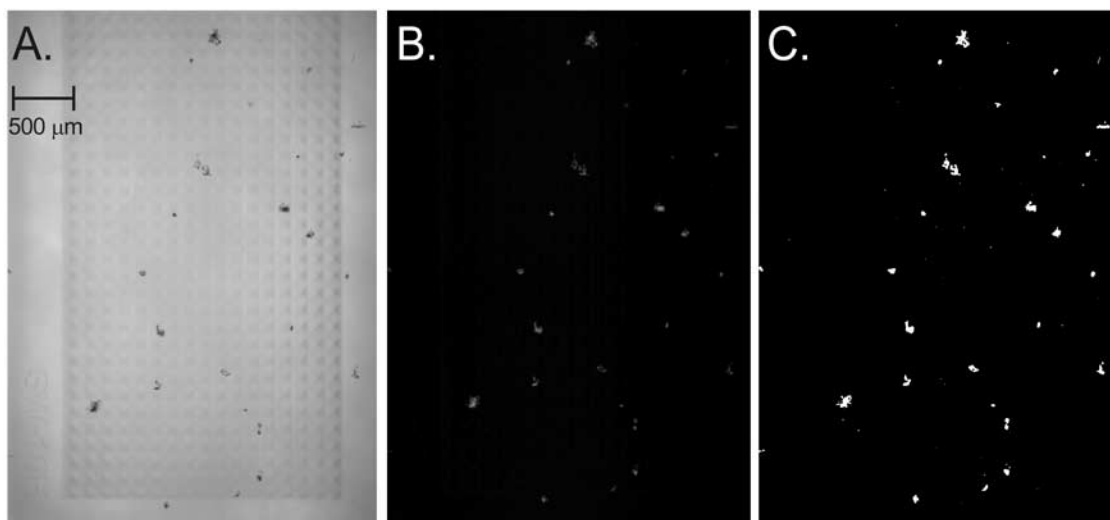
3.2. DFC Configuration and Processing

[14] We imaged floc using a digital single-lens reflex camera controlled remotely by a laptop computer. For the settling experiment, the resolution of each image was 14.50 μm per pixel, with a 4.13 cm $\times$ 6.22 cm field of view and a 2.5 cm depth of field. For the entrainment experiment, the resolution was 11.29 μm per pixel, with a 3.22 cm $\times$ 4.84 cm field of view and a 1.5 cm depth of field. Particles were defined by a minimum of three pixels, so the minimum resolvable floc diameter was 43.50 μm in the settling experiment and 33.87 μm in the entrainment experiment. Flocs were imaged (Figure 2) by silhouetting, or backlighting, to provide maximum contrast between the floc and the background [*Li and Ganczarczyk*, 1987; *Fennessy et al.*, 1994; *Manning and Dyer*, 2002]. Field trials revealed that while the opaque particles that comprise the bulk of the mass and volume of the floc population were resolved with our configuration, unflocculated fine material and translucent particles (e.g., free-floating bacteria [*Noe et al.*, 2007]) were not resolved. In a separate experiment at the same location, the majority of the suspended particle volume concentration measured by a LISST-100X (Sequoia Scientific, 1.25–250 μm size range) was larger than the minimum resolvable floc diameter of the DFC (G. Noe et al., unpublished data, 2006).

[15] In image processing, the two-dimensional projection of each floc was delineated from the background via image binarization (Figure 2), and perimeter, area, major and minor axes, eccentricity, equivalent spherical diameter, and spatial orientation were measured. As a first step toward digital image binarization and tabulation of floc properties, we subtracted a dark current image (averaged from 10 images acquired with the lens cap on before each experiment) and a background image (averaged from 10 images acquired in quiescent water with no suspended floc) from each raw gray scale image (Figures 2a and 2b). Images were then binarized by thresholding (Figure 2c) [*Mikkelsen et al.*, 2005]. Postbinarization, each image was checked by an operator to ensure that only in-focus flocs were binarized and that lighting conditions had a consistent effect on thresholding, and masks were created to remove bubbles and particles that adhered to the imaging equipment. A filter based on the aspect ratio of delineated particles automatically generated masks to remove nondetrital filaments of *Utricularia*. Once masked areas were removed from the binarized image, spatial statistics were computed for each particle, defined as a region of contiguous adjacent or diagonal "on" pixels.

[16] Assuming sphericity, two-dimensional geometric measurements from the binarized image were extrapolated to three dimensions, enabling the calculation of particle volumes and suspended floc concentrations. On the basis of image examination, Everglades flocs were better approximated as spheres than as cylinders, rods, or discs. Depending on particle eccentricity and orientation, the assumption of sphericity can underestimate or overestimate the volume of individual flocs but in a randomly oriented population produces low error overall. To calculate suspended floc concentration, we divided the computed spherical floc volumes by the control volume of the image [e.g., *Milligan*, 1996; *Belliveau et al.*, 1997; *Mikkelsen et al.*, 2005]. The

Figure 2. Processing sequence for floc images. (a) Original photograph, cropped. The grid in the background is a portion of the flash diffuser. (b) Image from Figure 2a with background and dark current field subtracted. (c) Binarized image, produced by thresholding the background-subtracted image in Figure 2b.
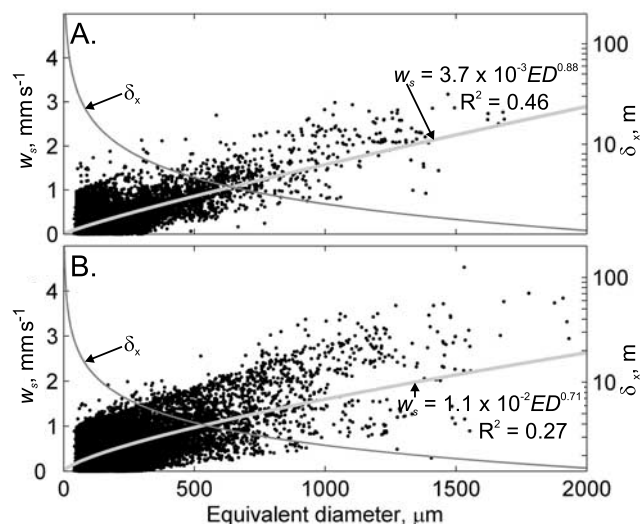
known field of view provided the upstream/downstream and top/bottom bounds of the control volume. Along the third dimension, the vertical face of the flash housing provided another bound, corresponding to the far side of the image's depth of field. The final bound in the third dimension of the control volume was delineated by the depth of field; out-of-focus flocs located outside the image volume were removed from images in the thresholding process.
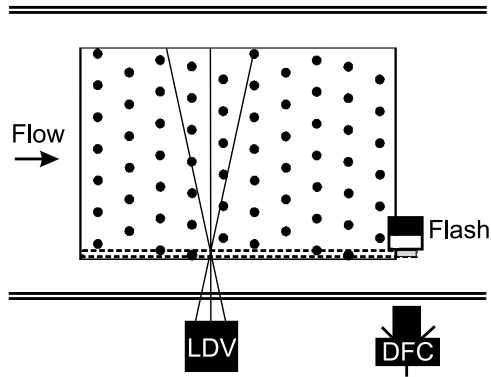
3.3.   Settling Column Experiment

[17] We performed settling experiments within 24 h of field collection in a thermally insulated, 5-cm inner diameter, square Plexiglas tube, 95 cm high. Viewing ports were located 35 cm from the top of the tube, which ensured that settling flocs had reached their terminal velocity. Thermal convection was negligible, evidenced by the lack of upward moving aggregates in all frames analyzed. Settling aggregates within the centered field of view were imaged stroboscopically at 1 Hz through the viewing ports. Aggregates were introduced over a 5-min span of time at a variable but low concentration by gently dragging a partially submersed, wide-mouthed (4.5 mm) pipette across the surface of the water. During and after introduction, 1000 frames were acquired over 17 min. After 1 h, another 100 frames were acquired, and 50 more frames were acquired after 2 h. A total of four runs (two replicates each for WCA-3A-5 aggregates and *Utricularia* site aggregates) were executed.

[18] To calculate floc settling velocities from the sequence of images, individual particles were identified and tracked from frame to frame. We developed an automated tracking code in Matlab that chose a match for a target floc from the population of flocs within a search area of the next frame on the basis of morphologic similarity, quantified by the multivariate Mahalanobis distance metric [*Hair et al.*, 1998]. The selected floc possessed the minimum Mahalanobis distance from the target floc. If none of the candidate flocs had a Mahalanobis distance below an operator-defined cutoff, no match was selected. If a match was found, the vertical fall distance, determined from the difference in the position of the centroid of the floc silhouette across frames, was computed and saved.

Often, an individual floc successfully tracked across 20 or more frames, and we averaged the fall distance per frame interval to produce a single point on the settling velocity versus equivalent diameter plot (Figure 3). The optimal vertical and horizontal dimensions of the search window, Mahalanobis distance cutoff value, and morphologic variables (equivalent spherical diameter, perimeter, major axis, and minor axis) used to compute Mahalanobis distance were determined by cali-

Figure 3. Mean settling velocity (w_s) versus aggregate equivalent diameter distributions for (a) the *Utricularia* site and (b) site WCA-3A-5, along with characteristic settling distances, δ_x. Mean settling velocities were measured by imaging aggregates in a settling column and digitally tracking individual aggregates across the sequence of frames. Each point represents a single aggregate and is associated with a standard deviation in settling velocity of 5×10^{-2} mm s^{-1} across multiple pairs of images. The characteristic settling distance here is defined as the downstream distance in 1 cm s^{-1} flow that entrained aggregates will travel while settling through 40 cm of open water column.

Figure 4. Top-view schematic of the racetrack flume and digital floc camera (DFC) configuration. The camera and flash are positioned opposite one another so that floc particles are silhouetted within the field of view (gray box). The flash housing forms one boundary of the image volume. On the camera side of the image volume, the boundary is not tangible but is defined as the location at which flocs become out of focus. In the dowel experiments, dowels (circles) are positioned in staggered rows within the sediment box. The laser Doppler velocimeter (LDV) sample volume is located between rows, where the three laser beam components (lines) intersect. The rectangle bounded by the dashed lines (which includes the image volume) denotes the control volume for the racetrack flume transport model (equation (7)).

bration against a manual tracking graphical user interface (GUI) [*Larsen*, 2008].

[19] Postprocessing analyses of the settling column data involved determining fractal dimensions and the relationships between equivalent diameter and settling velocity, porosity, and excess density for each sediment population. Approximating aggregates as spheres [*Fox et al.*, 2004], we assumed that Stokes' law applied to settling particles:

$$w_s = \frac{1}{18} ED^2 \left(\rho_f - \rho_w \right) \frac{g}{\mu}, \qquad (1)$$

where w_s is settling velocity, ED is particle equivalent diameter (computed as the diameter of a circle with area equivalent to the area of the digitized floc), ρ_f is the wet bulk density of the floc, ρ_w is water density, g is gravitational acceleration, and μ is the dynamic viscosity of water. Limitations of the application of Stokes' law to floc populations include the assumption of sphericity and the nonconstant nature of the excess density $(\rho_f - \rho_w)$, due to variation in floc porosity with equivalent diameter [*Tambo and Watanabe*, 1979]. Since excess density was an unknown function of equivalent diameter, we generalized equation (1) and used nonlinear regression to solve for the parameters c_1 and c_2 of the power law relationship:

$$w_s = c_1 ED^{c_2}. \qquad (2)$$

Using the calibrated values of c_1 and c_2, we solved for the excess density in equation (1) and determined floc porosity (θ):

$$\theta = \frac{\rho_p - \rho_f}{\rho_p - \rho_w}, \qquad (3)$$

where ρ_p is the particle density of the solid matter that comprises the aggregate. We assumed a typical organic matter particle density of 1.3 g cm^{-3} [*Cushing et al.*, 1993]. The porosity versus ED curve can be described by the relationship [*Logan and Wilkinson*, 1990]:

$$1 - \theta = c_3 ED^{c_4}, \qquad (4)$$

to which we fit coefficients c_3 and c_4 using nonlinear regression.

[20] Using the assumed particle density and a spherical volume based on equivalent diameter, we solved for the dry mass (m) of each aggregate:

$$m = \frac{\left(\rho_f - \rho_w \right) \rho_p}{6 \left(\rho_p - \rho_w \right)} \pi ED^3. \qquad (5)$$

Finally, we defined three fractal dimensions on the basis of aggregate geometry and settling statistics. Following *de Boer* [1997] and *Stone and Krishnappan* [2003], we defined a perimeter-area fractal dimension, D, as

$$p \sim A^{D/2}, \qquad (6)$$

where p is aggregate perimeter and A is aggregate area. A Euclidean object (e.g., a circle) has a D of unity, whereas fractal objects have higher values. *Logan and Wilkinson* [1990] have defined another fractal dimension, D_2, on the basis of the porosity-equivalent diameter relationship, where $D_2 = c_4 + 3$. For this fractal dimension, a D_2 of 3 is Euclidean, and fractal objects have lower values. Another fractal dimension, D_3, is derived from the exponent of the equivalent diameter-settling relationship, where $D_3 = c_2 + 1$ [*Logan and Wilkinson*, 1990].

3.4. Entrainment Experiments

[21] We performed two entrainment experiments in the racetrack flume at the Institute of Marine and Coastal Sciences, Rutgers University. Racetrack flumes are well suited for entrainment experiments because the test section is small compared to the path length for flow (thereby minimizing the effects of aggregation, disaggregation, and recirculated material on the suspended floc observed within the test section) and because flow does not pass through pumps that would break aggregates into smaller pieces with lower settling rates [*Nowell et al.*, 1989]. Baffles placed within the bends of the flume minimize secondary circulation. The test section, a 53 cm × 79 cm recessed sediment box, lies within a region of fully developed flow (C. Fuller, personal communication, 2006) on the side of the flume opposite the paddles that drive the flow.

[22] In the first experiment, the sediment box was filled with compacted peat overlain by approximately 2 cm of flocculated sediment to form a bed flush with the bottom of the flume. The total sediment thickness was 5 cm. This configuration represented a simplification of most Everglades slough environments, which have sparse rooted *Eleocharis* and *Bacopa* stems. Our modeled slough was more similar to the deepwater *Nymphaea* sloughs, which have little rooted vegetation. The second experimental configuration was more representative of Everglades ridge environments. We placed an array of dowels mounted to a Plexiglas plate

Table 1. Summary of Racetrack Flume Experiment Settings and Mean Floc Concentrations

	No Dowels			Dowels		
		Mean Steady State Floc Concentration			Mean Steady State Floc Concentration	
Interval	Depth-Averaged Velocity (cm s^{-1})	Mass (mg L^{-1})	Volume (μL L^{-1})	Depth-Averaged Velocity (cm s^{-1})	Mass (mg L^{-1})	Volume (μL L^{-1})
1	0.63	0.0076	0.098	1.4	0.012	0.12
2	1.4	0.0044	0.038	1.5	0.013	0.18
3	1.6	0.011	0.30	2.2	0.011	0.38
4	2.0	0.0018	0.015	2.4	0.0016	0.023
5	2.1	0.00030	0.0011	2.5	0.0020	0.035
6	2.0	0.00038	0.0021	2.7	0.0013	0.012
7	2.3	0.0029	0.076	3.0	0.0040	0.098
8	2.7	0.0037	0.18	3.2	0.022	0.64
9	3.5	0.062	3.3	3.8	0.090	3.6
10	4.2	0.013	0.96	4.8	0.19	11
11	5.1	0.049	3.2	5.9	0.52	27
12	5.8	0.061	2.1	6.8	0.81	39
13	6.2	0.13	5.0	7.2	0.95	41
14	6.2	0.27	16	7.8	0.93	43
15	6.4	1.9	93	7.8	4.6	270
16	8.1	14	810	12.3	5.2	200

within the sediment box (Figure 4) and formed the peat bed around the dowels. As in the "no-dowels" experiment, we added the floc over the peat bed so that the surface was flush with the flume bottom. The diameter (10 mm) and spacing (7.58 cm) of the dowels closely approximated the mean diameter and spacing of sawgrass stems at site WCA-3A-5, measured in August 2005 in 0.25 m^2 clip plots. The dowels protruded through the water surface and were placed in rows perpendicular to the flow, staggered so that every fifth row aligned. During both runs, the water depth was 15 cm. Flocculated sediment beds settled for 24 h prior to experimentation.

[23] Each of the two experiments consisted of 16 runs at different flume speeds (Table 1). Within the test section, a two-component Dantec laser Doppler velocimeter (LDV) operating in backscatter mode monitored flow velocities in the vertical and longitudinal (i.e., parallel to flow) directions with a validation rate of 80–100%. The LDV measurement volume, sampling flow over a region that was a source of the particles imaged by the DFC, was located over the sediment box, 10 cm from the wall and 32 cm from the upstream edge of the box (Figure 4). During each flume run, the LDV sampled a vertical profile of 10 logarithmically spaced points (auxiliary material), acquiring data for 10 min per point, which test runs revealed to be sufficient for flow statistics to converge to within less than 5% of their asymptotic values [*Larsen*, 2008].[1] Simultaneously, the DFC acquired 266 images of entrained sediment for each flume velocity at 1/6 Hz. The upstream edge of the image area coincided with the downstream edge of the sediment box, with the lower edge of the images located 1 cm above the flocculated sediment bed (Figure 4).

3.5. Analytical Postprocessing for Entrainment Experiment

[24] To determine the relationship between local hydraulics and floc entrainment, entrainment flux (J_e, g cm^{-2} s^{-1})
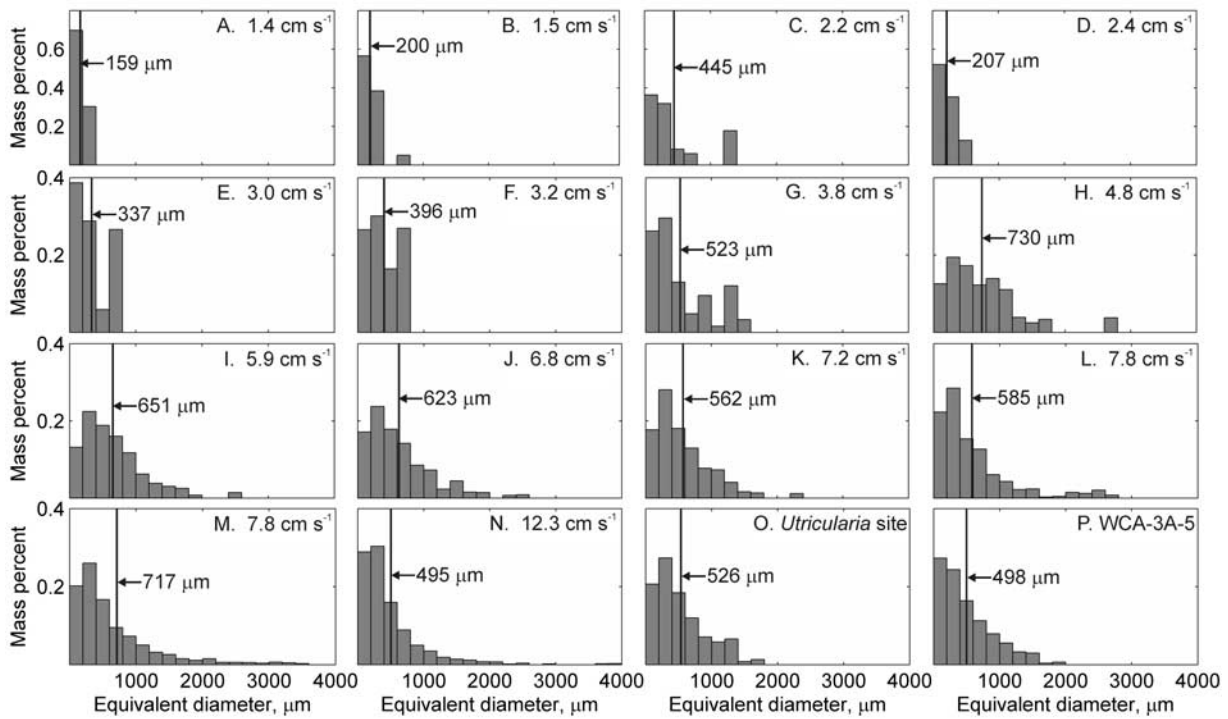
was compared to the bed shear stress at each flume speed. We determined bed shear stress from measured Reynolds stress profiles. Near the bed, the Reynolds stress, $\overline{\rho_w u'v'}$, attains its maximum value and approximates the bed shear stress [*Middleton and Wilcock*, 1994]. Here, u' and v' are the instantaneous perturbations from the time-averaged longitudinal and vertical flow velocities, respectively, and the overbar denotes a time average. Reynolds stress profiles conformed to the theoretical shape for most runs (auxiliary material).

[25] Entrainment flux was calculated from imaged floc concentrations and a transport model. The concentration C of floc within size class bin i at the longitudinal spatial coordinate x within the racetrack flume is described by

$$\frac{\partial C_i}{\partial t} + \bar{u}\frac{\partial C_i}{\partial x} = K\frac{\partial^2 C_i}{\partial z^2} + w_s\frac{\partial C_i}{\partial z}, \qquad (7)$$

where $\bar{u}$ is the time-averaged longitudinal velocity, z the vertical coordinate, t the time coordinate, K the eddy diffusivity, and w_s the settling velocity of the median floc diameter within i. Simplifying assumptions of this model consist of one-dimensional plug flow (i.e., no longitudinal dispersion over the short spatial scale of the sediment box), negligible recirculation of floc (i.e., a no-flux upstream boundary condition for sediment), a negligible reaction term over the spatial scale of the sediment box (i.e., no aggregation or disaggregation), and steady flow. The entrainment flux J_e is the ultimate source of floc and appears in the lower boundary condition: a specified flux equal to $J_e - w_s C_{i,z\min}$ at the bed, where $C_{i,z\min}$ is the floc concentration in the bottom cell of the model domain. By specifying K and the remaining boundary conditions (no flux at the water surface and a specified flux equal to $\bar{u}C_{i,x\max}$ at the downstream boundary, where $C_{i,x\max}$ is the floc concentration at the extreme downstream cell of the model domain), we optimized J_e using a Levenberg-Marquardt algorithm that minimized the error between observed concentrations in the image area and modeled concentrations.

Figure 5. Floc size distribution histograms for (a–n) the racetrack flume experimental run with dowels and for the aggregate populations observed in the settling experiment for (o) the *Utricularia* site and (p) site WCA-3A-5, which are representative of the floc bed for each site. The bin width is 200 μm, and vertical lines represent the mass-weighted mean equivalent diameter for each distribution. Floc masses were computed by converting aggregate areas into assumed spherical volumes, which were then converted to mass using Stokes' law and the settling column results (equations (1)–(5)). Two intervals (intervals 5–6 in Table 1) of the racetrack experiment in which entrained flocs were all of the lowest size class are not depicted.

[26] To compute vertical profiles of K, we assumed a turbulent Schmidt number of unity, which is valid for low concentrations of fine suspended sediment [*Shiono et al.*, 2003; *Toorman*, 2003; *Fu et al.*, 2005]. We then determined K from LDV data at each profile location in accordance with the turbulent viscosity hypothesis [*Pope*, 2000]:

$$\overline{u'v'} = -K\frac{\partial \bar{u}}{\partial z}. \qquad (8)$$

K values for intermediate locations in the water column were linearly interpolated from the sampled points, excluding the occasional negative computed value.

[27] At each test value of J_e, equation (7) was solved over the model domain, which extended from the bed to the water surface in the vertical dimension and from the upstream end of the sediment box to the downstream end of the image area in the longitudinal dimension (Figure 4). Equation (7) was discretized and solved using a transient forward difference algorithm that ran until $\partial C_i/\partial t$ converged to zero. Spatial ($\Delta z = 1$ mm and $\Delta x = \Delta t \times \langle \bar{u} \rangle$, where the angle brackets denote a depth averaged quantity) and time ($\Delta t = 0.5$ ms) steps were selected to ensure stability and convergence. Comparing the steady state floc concentration at the DFC image location to the measured concentration, the Levenberg-Marquardt algorithm adjusted J_e until the error between measured and modeled concentration was

minimized. This solution procedure was repeated for 14 different size class bins, each spanning 250 μm. Uncertainty in the optimized values of J_e arises from uncertainty in K, uncertainty and variability in the measured w_s, instantaneous turbulence, and stochasticity in particle entrainment, the latter of which increases with particle size because of the relative rarity of large particles within the floc bed.

4. Results and Discussion

4.1. Morphologic and Settling Characteristics of Everglades Floc

[28] The settling velocity of Everglades aggregates exhibited a positive trend with equivalent diameter (Figure 3). High scatter, typical for unbinned floc equivalent diameter/settling velocity relationships [*Droppo*, 2004; *Curran et al.*, 2007] and especially present at high velocities, arises largely from variability in floc shape and pore configuration. In this experiment aggregates from site WCA-3A-5, in which floating mats of *Utricularia* and periphyton were absent, exhibited less variability in settling velocity ($R^2 = 0.27$) than aggregates from the *Utricularia* site ($R^2 = 0.46$). Aggregates from the two sites also differed significantly in both their settling velocity and equivalent diameter (Figures 5o and 5p) distributions (Kolmogorov-Smirnov tests, $p < 0.001$, $N_{Utricularia} = 20,288$, $N_{WCA-3A-5} = 57,519$), and the 95% confidence intervals bracketing the

Table 2. Fractal Dimensions of Everglades Flocculated Bed Sediment Compared to Floc From Other Environments[a]
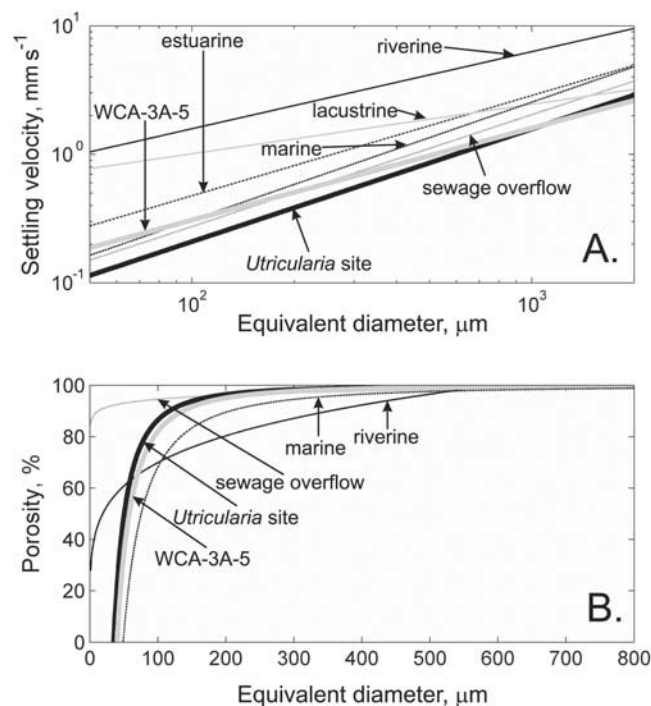
Floc Population	D	D_2	D_3	Source
Euclidean object	1.0	3.0	3.0	
Utricularia site	1.27 ± 0.01	1.08 ± 0.06	1.88 ± 0.01	this study
WCA-3A-5	1.34 ± 0.00	1.13 ± 0.04	1.71 ± 0.01	this study
Estuarine			1.78	*Gibbs* [1985]
Estuarine		2.0–3.0		*Winterwerp et al.* [2002]
Riverine	1.25–1.44			*de Boer* [1997]
Riverine	1.25–1.36			*Stone and Krishnappan* [2003]
Riverine			1.6	*Droppo* [2004]
Lacustrine			1.39–1.69	*Hawley* [1982]
Marine snow		1.24–1.71	1.26 ± 0.06	*Alldredge and Gotschalk* [1988]
Sewage overflow			1.87	*Droppo* [2004]
Bioreactor, normal		1.3		*Tambo and Watanabe* [1979]
Bioreactor, filamentous		1.0		*Tambo and Watanabe* [1979]
Lab, natural organic acid extract	1.29–1.33		1.91–1.99	*Aouabed et al.* [2008]

[a]Error values, where given, are 95% confidence intervals.

parameter estimates in equation (2) did not overlap. Likewise, the confidence intervals bounding the estimates of D and D_3 did not overlap (Table 2). D was less Euclidean for WCA-3A-5 ($D = 1.34 ± 0.00$) than for the *Utricularia* site ($1.27 ± 0.01$), indicating that WCA-3A-5 had aggregates with more convoluted boundaries. Similarly, D_3 was less Euclidean for site WCA-3A-5 ($D_3 = 1.71 ± 0.01$) than for the *Utricularia* site ($D_3 = 1.88 ± 0.01$), indicating that the aggregate wet density decreased at a faster rate with increasing diameter for site WCA-3A-5. Still, changes in porosity with particle diameter were similar between the two sites, as evidenced by the overlapping 95% confidence intervals for D_2 ($1.13 ± 0.04$ and $1.08 ± 0.06$ for WCA-3A-5 and the *Utricularia* site, respectively). Differences in the morphology of aggregate populations from the two sites were likely related to the abundance of periphyton at the *Utricularia* site relative to site WCA-3A-5. Periphyton can be an important source of EPS and other compounds that bind aggregates [*Wotton*, 2005] and likely plays a substantial role in floc and suspended particle formation in the Everglades [*Noe et al.*, 2007]. Differences in aggregate morphology between the two WCA-3A sites suggest that as the organic content and microbial composition of water bodies change (e.g., from urbanization, climate change, recovery from acidification), transport properties of particulate organic matter will likewise change.
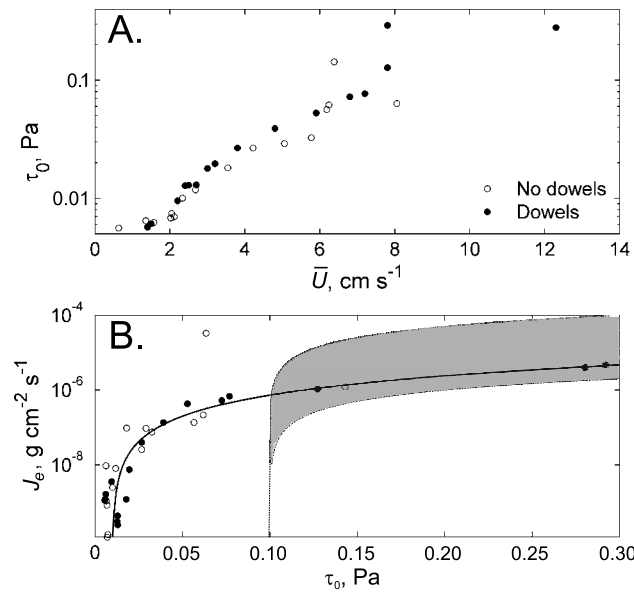
[29] Compared to floc from other aquatic environments, Everglades aggregates had among the lowest settling velocities over the continuum of particle sizes (Figure 6a), with values close to those of sewage and marine flocs, two other highly organic floc populations. However, the slope of the settling velocity/equivalent diameter curve on log-log axes (Figure 6a and Table 2) was greater (i.e., more Euclidean) for Everglades aggregates (0.71–0.88) than for most other floc (0.26–0.78) except for other highly organic floc from sewage overflow and from natural organic acid extracts artificially flocculated in the lab (0.87–0.99). This placement of Everglades aggregates, sewage overflow flocs, and flocs of natural organic acid extracts on one extreme of the gradient in settling velocity is due to the almost purely organic nature of these flocs and to their relatively high porosity over the most abundant size classes (Figure 6b). These characteristics lead to wet bulk and particle densities that are exceedingly low, producing the observed low settling velocities [e.g., *Wotton and Warren*, 2007]. Simi-

larly, because even the smaller Everglades floc particles (~100 μm) have relatively high porosities (~90%) and low wet bulk densities (Figure 6b), further addition of organic matter to form larger particles does not greatly change overall porosity and wet density compared to the addition of matter to more predominantly inorganic floc, resulting in a relatively high D_3 for Everglades and other organic floc. Biostabilization by EPS at the scale of the individual floc particle may have further contributed to the high porosities, low wet densities, and low settling velocities of Everglades aggregates relative to more inorganic floc.

Figure 6. Comparison of (a) settling velocity and (b) porosity relationships for Everglades flocculated bed sediment and floc from estuarine [*Gibbs*, 1985] (Chesapeake Bay), riverine [*Droppo*, 2004] (14-Mile Creek and 16-Mile Creek, Milton, Ontario), lacustrine [*Hawley*, 1982] (Lake Michigan), marine [*Fennessy et al.*, 1994], and sewage overflow [*Droppo*, 2004] (Milton, Ontario) environments.

Figure 7. Racetrack flume experiment floc entrainment results. (a) Relationship between bed shear stress (τ_0) and depth-averaged velocity ($\bar{U}$) in the experimental runs with and without dowels. Except for at high velocities where large amounts of sediment are entrained, bed shear stresses are lowest in the configuration without dowels. (b) Entrainment flux J_e as a function of bed shear stress. The solid line is the fitted regression describing the entrainment relationship (equation (9)), excluding the outlier. The shaded region depicts the range of typical entrainment fluxes for inorganic flocs [*Winterwerp and van Kesteren*, 2004].

[30] The two populations of Everglades floc also had D_2 values that were lower (less Euclidean) than those of floc from more turbulent environments (Table 2). These low D_2 values arise from the persistence in the Everglades of large, porous flocs that would disaggregate by shearing in higher-energy environments [*Eisma*, 1986; *Khelifa and Hill*, 2006]. As the experimental results of *Larsen et al.* [2009] show, periods of high shear in the predominantly low-shear wetland environment primarily cause aggregation rather than disaggregation, resulting in large, weak, porous flocs. These weak flocs can persist because of the abundance of microbial EPS in wetlands, which increases floc cohesion [*Droppo et al.*, 1997]. In contrast, in most other aquatic environments, relatively high shear, turbulence, and potentially less abundant EPS limit floc size [*Mehta and Partheniades*, 1975; *Krone*, 1978; *Hill et al.*, 2001], settling fluxes, and the persistence of weak flocs [*Partheniades*, 1977; *Lick et al.*, 1992; *Wolanski*, 1995].

4.2. Entrainment of Everglades Floc

[31] Consistent with findings that the presence of emergent stems can increase secondary circulation currents [*Nepf and Koch*, 1999] and turbulence production [*Nepf*, 1999] relative to an open water column, Reynolds stresses near the bed ($\approx \tau_0$) were higher for the entrainment experiment in which dowels were present than for the experiment without dowels (Figure 7a). However, as a function of τ_0, entrainment rates in both experiments collapsed onto a single curve

with the exception of one high-J_e outlier (Figure 7b), which resulted from the entrainment and saltation of a few large pieces of peat and litter during the run. The form of the commonly used relationship for floc entrainment is

$$J_e = \max\left[M\left(\frac{\tau_0 - \tau_e}{\tau_e} \right)^n, 0 \right], \qquad (9)$$

where M and n are regression coefficients, τ_0 is bed shear stress, and τ_e is the critical bed shear stress at the point of entrainment [*Winterwerp and van Kesteren*, 2004]. Excluding the outlier in Figure 7b as an artifact of an incompletely compacted floc bed, the coefficients for the overall entrainment curve for the racetrack flume experiments were $M = 2.2 \times 10^{-8}$ g cm^{-2} s^{-1}, $n = 1.6$, and $\tau_e = 1.0 \times 10^{-2}$ Pa. Thus, below a threshold shear stress of 1.0×10^{-2} Pa, floc was entrained at a negligibly low rate. Above this threshold J_e increased rapidly at a rate that slowed with further increases in bed shear stress.

[32] Through the 1.75–2.0 mm size class, entrainment curves were sufficiently distinct to fit values of M, τ_e, and n for each size class (Table 3). For larger size classes, entrainment curves followed no distinct trend because of the limited numbers of large flocs within the bed and the stochastic nature of their entrainment. While fitted τ_e values can be misleading for larger floc sizes because of the small number of points near the size class-specific threshold, the minimum τ_0 values at which entrainment was observed for each size class (Table 3) show that larger size classes require larger bed shear stresses for entrainment. This phenomenon is also apparent in particle size histograms for each flume speed (Figure 5) and is consistent with a mechanism of surface erosion of floc held together by interparticle electrochemical bonds rather than mass erosion or bed fluidization [*Zreik et al.*, 1998].

[33] While the entrainment of larger particles increases with increasing bed shear stress, at a bed shear stress of 2.0×10^{-2} Pa, the floc size classes that contain the majority of the mass within the bed are all in suspension, and the mass-weighted mean equivalent diameter and distribution of equivalent diameters converge upon those of the bed population (assuming that the distribution of floc for the *Utricularia* site settling experiment is representative of the bed population) and remain roughly constant (Figure 5). Although the low abundance and relatively low bulk density of the largest flocs limit their contribution to the total mass of floc in suspension, large flocs substantially contribute to the volume of suspended material. At shear stresses above the entrainment threshold, the mean volumetric J_e increases from the smallest size class to the largest size classes (Table 3), but in terms of mass the 250–500 μm size class is the dominant contributor to the population of particles in suspension.

[34] The critical shear stress for entrainment of Everglades floc is an order of magnitude lower than is typical for environments with predominantly inorganic floc (Table 3), suggesting that the biostabilization did not substantially strengthen interactions between flocs. However, because M (equation (9)) is also an order of magnitude lower for Everglades floc than for other floc populations, the entrainment rate of Everglades floc lies within the range of typical values at relatively high bed shear stresses (0.15–0.30 Pa,

Table 3. Entrainment Statistics for Everglades Floc and Typical, Less Organic Floc

Population	Minimum τ_0 at Which Entrainment Observed (Pa × 10⁻²)	M		τ_e		n		Mean J_e Above Entrainment Threshold	
		Mass Regression (g cm⁻² s⁻¹ × 10⁻⁹)	Volume Regression (mL cm⁻² s⁻¹ × 10⁻⁷)	Mass Regression (Pa × 10⁻²)	Volume Regression (Pa × 10⁻²)	Mass Regression	Volume Regression	Mass Regression (g cm⁻² s⁻¹ × 10⁻⁷)	Volume Regression (mL cm⁻² s⁻¹ × 10⁻⁵)
Typical [*Winterwerp and van Kesteren*, 2004]		100−5000		10−500		1			
Everglades, bulk population	0.56	22	6.2	1.0	0.9	1.6	1.9	6.1	4.6
Everglades, 0−250 μm	0.56	3.1	0.28	1.0	1.0	1.8	1.8	1.4	0.14
Everglades, 250−500 μm	0.56	4.9	1.1	1.0	1.0	1.6	1.7	1.6	0.40
Everglades, 500−750 μm	0.56	6.7	5.1	1.1	1.3	1.4	1.3	1.2	0.58
Everglades, 750−1000 μm	0.62	3.4	2.0	0.9	0.7	1.4	1.3	0.92	0.64
Everglades, 1.00−1.25 mm	1.8	6.5	2.7	1.1	0.6	1.2	1.2	0.75	0.68
Everglades, 1.25−1.5 mm	0.95	3.0	12	0.8	1.7	1.2	1.0	0.52	0.63
Everglades, 1.5−1.75 mm	2.7	5.9	7.2	0.9	1.0	0.90	0.98	0.50	0.70
Everglades, 1.75−2.0 mm	3.9	0.051	0.054	0.2	0.1	1.5	1.4	0.35	0.61
Everglades, 2.0−2.25 mm	2.9							0.90	1.5
Everglades, 2.25−2.5 mm	6.4							0.65	1.3
Everglades, 2.5−2.75 mm	2.7							0.51	1.2
Everglades, 2.75−3.0 mm	140							0.46	1.4
Everglades, 3.0−3.25 mm	130							0.62	1.8
Everglades, 3.25−3.5 mm	6.2							0.71	2.2

Figure 7b). Even so, floc entrainment events are rare in the present-day Everglades, where average bed shear stresses (1.0×10^{-7} Pa to 4.9×10^{-4} Pa, from the u_* data provided by *Harvey et al.* [2008]) typically lie well below the 1.0×10^{-2} Pa threshold for floc entrainment. Thus, in the Everglades and other wetlands with typically low bed shear stresses that are near the entrainment threshold, the entrainment of bed sediment will be a far more critical control on suspended floc dynamics than in other aquatic environments, where aggregation and disaggregation instead exert the primary control over floc size.

4.3. Extending Laboratory Experimental Results to the Field Setting: Implications for Particle Transfer

[35] Often, implications of laboratory studies of floc cannot be directly extended to the field because of the structural disruption of flocs that occurs during sample collection [*Grant and Gust*, 1987; *Alldredge and Gotschalk*, 1988]. While morphologic characteristics of Everglades floc beds measured in the field [*Larsen et al.*, 2009] differed from those in our laboratory experiments, the differences were small. For instance, bulk densities of floc beds in the field ($N = 1$ core) and in a laboratory flume ($N = 1$ core) 24 h after floc introduction were 1.3×10^{-2} g cm⁻³ and 8.4×10^{-3} g cm⁻³, respectively. Likewise, the mean mass-weighted equivalent diameter of floc observed over 18.5 h in the field was 262 ± 130 μm, which is comparable to the mean equivalent diameter of entrained floc during the low-velocity runs of the racetrack flume experiment (159–200 μm, Figure 5). The fractal dimension D of floc observed in the field (1.37–1.43) was approximately equal to the D of floc in the flume experiment (1.37–1.41), supporting the technique of allowing floc to settle for 24 h in the flume to form an aggregated, deposited bed. However, the D of aggregates in the settling experiment (1.27–1.34, Table 2), was slightly lower than that of field floc, indicating that some structural disruption as a result of shear occurred in the aggregate collection and transfer process.

[36] Physical sampling of aggregates biases settling column results by preferentially breaking large, weak, porous flocs into smaller pieces and by artificially compacting flocs against the container walls, which both increase the relative abundance of compact flocs that settle rapidly. Despite this bias, above a floc equivalent diameter of 100 μm, Everglades floc observed during the settling experiments was significantly more porous than marine or riverine floc (Figure 6b), had a less Euclidean D_2 value, and over the full range of particle sizes, settled more slowly than less organic populations. Thus, these qualitative comparisons of settling velocity and porosity between organic and inorganic floc populations obtained from laboratory analysis will extend to the field setting.

[37] Field experiments have shown that biofilms coating benthic substrata can cause a higher τ_e than that measured in laboratory entrainment experiments [*Grant and Gust*, 1987]. Hence, the 1.0×10^{-2} Pa threshold for entrainment of Everglades floc is a lower bound for τ_e in field conditions, which further emphasizes the rarity of floc entrainment events in the present-day system. While the lower bound on the shear stress needed to entrain this highly organic floc population remains an order of magnitude lower than that needed to entrain more inorganic floc (Figure 7b), additional field experimentation is needed to close the upper bound on the actual Everglades floc entrainment threshold. Although the laboratory entrainment threshold potentially underestimates the threshold shear stress in the field, laboratory entrainment fluxes (Figure 7b) provide an upper bound for J_e in the field and represent peak entrainment rates. Erosion of floc beds in the field will eventually expose sediment that is more consolidated than surface sediment and erodes at a slower rate absent further increases in shear stress [*Amos et al.*, 1992].

[38] Vegetation rooted in the substratum additionally influences floc entrainment in the field setting. Although our racetrack flume experiments with and without dowels suggest that vegetation does not alter τ_e (Figure 7b), the presence of stem wakes alters flow hydraulics and the

depth-averaged velocity at which sediment is entrained (Figure 7a). However, whether emergent vegetation increases or decreases bed shear stresses and organic floc entrainment in a particular setting requires flow modeling, for the effects of secondary circulation and turbulence production in stem wakes [*Nepf*, 1999; *Nepf and Koch*, 1999] compete with the effects of stem drag, which slows mean flow velocities [*Kadlec*, 1990; *Nepf*, 1999].

[39] Overall, the lower settling velocities and lower threshold shear stress for entrainment of Everglades floc imply that the highly organic floc commonly found in wetlands and floodplains is more mobile than less organic floc because of its high porosity and low wet density. However, coupled to a low threshold shear stress for organic floc entrainment are the characteristically low flows and bed shear stresses of wetlands and floodplains. Thus, in contrast to rivers and streams, where transport of floc is an important means of redistributing organic carbon and nutrients but is often supply limited [*Cushing et al.*, 1993], floc transfer is often transport-limited in slowly flowing aquatic environments, where suspended floc concentrations and deposition rates will be governed largely by the balance between settling and entrainment. In contrast, turbulent fluxes of particles to the bed dominate deposition in streams [*Newbold et al.*, 2005].

[40] In wetlands and floodplains, where low shear stresses permit coexistence of a range of floc sizes including relatively weak, porous, and large flocs, settling velocities affect floc spiraling distances and the influence of floc on ecosystem metabolism. Small particles, which settle slowly compared to large particles and tend to be relatively enriched in nutrients in the Everglades [*Noe et al.*, 2007], with faster nutrient uptake times [*Noe et al.*, 2003], have a long characteristic distance of travel before settling to the benthos (Figure 3) and a potentially large effect on water column metabolism. In contrast, less labile large flocs have a shorter characteristic travel distance, a higher probability of immobilization in the benthos, and may contribute more to the development of peat soils. If production and entrainment of floc particles is patchy, the deposition of large floc particles is also likely to be patchy relative to the deposition of small particles because of differences in water column residence times and characteristic travel distances. Thus, large flocs potentially have a greater influence on the development of local microtopography than small flocs in peatlands such as the Everglades.

[41] Where slowly flowing aquatic environments abut more turbulent water bodies and bed shear stresses are high, the relative mobility of organic floc has further implications for ecosystem processes and mass transfer. For example, highly organic coastal marsh floc may become entrained further inland than less organic floc, affecting the position of the coastal marsh front or its resilience to storms. Also, because of its lower settling velocity, organic wetland floc entrained within the margins of riparian zones will generally be transported further downstream than less organic floc before incorporation into the benthos, providing a longer water column residence time for processing and potentially a greater influence on water column metabolism [e.g., *Meyer and Edwards*, 1990; *Wetzel*, 1995; *Battin et al.*, 2008]. However, in lakes fringed by wetlands, wetland flocs with low settling velocities can be transported further

into the lake interior than less organic flocs, increasing their probability of settling into the anaerobic hypolimnion and of long-term immobilization.

5. Conclusions

[42] Floc collected from two sites in the Everglades with different coverage of floating periphyton mats exhibited different morphology, with floc from the *Utricularia* site (abundant periphyton) shifted to larger-diameter size distributions, higher porosity, and lower settling velocities than floc from WCA-3A-5. Differences were likely due to the abundance and character of microbial EPS, with floc from the *Utricularia* site having more abundant EPS available to bind detrital fragments. Morphodynamic differences between Everglades floc populations were nonetheless small compared to differences between the highly organic Everglades floc and more inorganic floc from lakes, estuaries, and rivers. Namely, Everglades floc generally had lower settling velocities and higher porosity than inorganic floc and was entrained at substantially lower bed shear stresses. On the basis of the similarities between Everglades floc and other organic floc and on the experiments presented here, highly organic floc is more mobile than less organic floc, which has implications for ecosystem metabolism, materials cycling, and even landscape evolution.

[43] Despite the low threshold shear stress for the entrainment of highly organic floc, shear stresses in wetlands and other floodplain and shallow aquatic ecosystems often lie below the entrainment threshold, producing transport-limited conditions. In the present-day Everglades, the lower-bound entrainment threshold of 1.0×10^{-2} Pa is rarely exceeded. Restoration efforts designed to increase floc transport would therefore need to increase flow velocities and bed shear stresses. Further numerical modeling and field experimentation are needed to determine how different restoration scenarios would affect bed shear stresses in different vegetation communities and to establish an upper bound on floc entrainment thresholds where benthic microbial colonization is high.

References

Alldredge, A. L., and C. Gotschalk (1988), In situ settling behavior of marine snow, *Limnol. Oceanogr.*, *33*, 339–351.

Alldredge, A. L., and M. W. Silver (1988), Characteristics, dynamics and significance of marine snow, *Prog. Oceanogr.*, *20*, 41–82, doi:10.1016/0079-6611(88)90053-5.

Amos, C. L., G. R. Daborn, H. A. Christian, A. Atkinson, and A. Robertson (1992), In situ erosion measurements on fine-grained sediments from the Bay of Fundy, *Mar. Geol.*, *108*, 175–196, doi:10.1016/0025-3227(92)90171-D.

Aouabed, A., D. E. Hadj Boussaad, and R. Ben Aim (2008), Morphological characteristics and fractal approach of the flocs obtained from the natural

organic matter extracts of water of the Keddara dam (Algeria), *Desalination*, 231, 314–322, doi:10.1016/j.desal.2007.11.050.

Battin, T. J., L. A. Kaplan, J. D. Newbold, and C. M. E. Hansen (2003), Contributions of microbial biofilms to ecosystem processes in stream mesocosms, *Nature*, 426, 439–442, doi:10.1038/nature02152.

Battin, T. J., L. A. Kaplan, S. Findlay, C. S. Hopkinson, E. Marti, A. I. Packman, J. D. Newbold, and F. Sabater (2008), Biophysical controls on organic carbon fluxes in fluvial networks, *Nat. Geosci.*, 1, 95–100, doi:10.1038/ngeo101.

Belliveau, D. J., T. G. Milligan, G. D. Youle, B. D. Beanlands, and A. Trivett (1997), MIMS—Moored Impact Monitoring System, in *Oceans 97 MTS/IEEE Conference Proceedings*, vol. 1, pp. 391–396, Inst. of Electr. and Eletron. Eng., Piscataway, N. J.

Blanchard, G. F., et al. (2000), The effect of geomorphological structures on potential biostabilisation by microphytobenthos on intertidal mudflats, *Cont. Shelf Res.*, 20, 1243–1256, doi:10.1016/S0278-4343(00)00021-2.

Christiansen, T., P. L. Wiberg, and T. G. Milligan (2000), Flow and sediment transport on a tidal salt marsh surface, *Estuarine Coastal Shelf Sci.*, 50, 315–331, doi:10.1006/ecss.2000.0548.

Curran, K. J., P. S. Hill, T. G. Milligan, O. A. Mikkelsen, B. A. Law, X. Durrieu de Madron, and F. Bourrin (2007), Settling velocity, effective density, and mass composition of suspended sediment in a coastal bottom boundary layer, Gulf of Lions, France, *Cont. Shelf Res.*, 27, 1408–1421, doi:10.1016/j.csr.2007.01.014.

Cushing, C. E., G. W. Minshall, and J. D. Newbold (1993), Transport dynamics of fine particulate organic matter in two Idaho streams, *Limnol. Oceanogr.*, 38, 1101–1115.

D'Alpaos, A., S. Lanzoni, M. Marani, and A. Rinaldo (2007), Landscape evolution in tidal embayments: Modeling the interplay of erosion, sedimentation, and vegetation dynamics, *J. Geophys. Res.*, 112, F01008, doi:10.1029/2006JF000537.

de Boer, D. H. (1997), An evaluation of fractal dimensions to quantify changes in the morphology of fluvial suspended sediment particles during baseflow conditions, *Hydrol. Processes*, 11, 415–426, doi:10.1002/(SICI)1099-1085(19970330)11:4<415::AID-HYP450>3.0.CO;2-W.

Droppo, I. G. (2003), A new definition of suspended sediment: Implications for the measurement and prediction of sediment transport, in *Erosion and Sediment Transport Measurement in Rivers: Technological and Methodological Advances*, edited by J. Bogen, T. Fergus, and D. E. Walling, *IAHS Publ.*, vol. 283, pp. 3–12.

Droppo, I. G. (2004), Structural controls on floc strength and transport, *Can. J. Civ. Eng.*, 31, 569–578, doi:10.1139/l04-015.

Droppo, I. G., and E. D. Ongley (1992), The state of suspended sediment in the freshwater fluvial environment: A method of analysis, *Water Res.*, 26, 65–72, doi:10.1016/0043-1354(92)90112-H.

Droppo, I. G., and E. D. Ongley (1994), Flocculation of suspended sediment in rivers of southeastern Canada, *Water Res.*, 28, 1799–1809, doi:10.1016/0043-1354(94)90253-4.

Droppo, I. G., G. G. Leppard, D. T. Flannigan, and S. N. Liss (1997), The freshwater floc: A functional relationship of water and organic and inorganic floc constituents affecting suspended sediment properties, *Water Air Soil Pollut.*, 99, 43–54.

Eisma, D. (1986), Flocculation and de-flocculation of suspended matter in estuaries, *Neth. J. Sea Res.*, 20, 183–199, doi:10.1016/0077-7579(86)90041-4.

Eisma, D., T. Schuhmacher, H. Boekel, J. VanHeerwaarden, H. Franken, M. Laan, A. Vaars, F. Eijgenraam, and J. Kalf (1990), A camera and image-analysis system for in situ observation of flocs in natural waters, *Neth. J. Sea Res.*, 27, 43–56, doi:10.1016/0077-7579(90)90033-D.

Fagherazzi, S., M. Marani, and L. K. Blum (2004), Introduction: The coupled evolution of geomorphological and ecosystem structures in salt marshes, in *The Ecogeomorphology of Tidal Marshes, Coastal Estuarine Stud.*, vol. 59, edited by S. Fagherazzi, M. Marani, and L. K. Blum, pp. 1–4, AGU, Washington, D. C.

Fennessy, M. J., K. R. Dyer, and D. A. Huntley (1994), INSSEV: An instrument to measure the size and settling velocity of flocs in situ, *Mar. Geol.*, 117, 107–117, doi:10.1016/0025-3227(94)90009-4.

Fox, J. M., P. S. Hill, T. G. Milligan, A. S. Ogston, and A. Boldrin (2004), Floc fraction in the waters of the Po River prodelta, *Cont. Shelf Res.*, 24, 1699–1715, doi:10.1016/j.csr.2004.05.009.

Fu, X., G. Wang, and X. Shao (2005), Vertical dispersion of fine and course sediments in turbulent open-channel flows, *J. Hydraul. Eng.*, 131, 877–888, doi:10.1061/(ASCE)0733-9429(2005)131:10(877).

Furukawa, K., E. Wolanski, and H. Mueller (1997), Currents and sediment transport in mangrove forests, *Estuarine Coastal Shelf Sci.*, 44, 301–310, doi:10.1006/ecss.1996.0120.

Gibbs, R. J. (1985), Estuarine flocs: Their size, settling velocity and density, *J. Geophys. Res.*, 90, 3249–3251, doi:10.1029/JC090iC02p03249.

Grant, J., and G. Gust (1987), Prediction of coastal sediment stability from photopigment content of mats of purple sulphur bacteria, *Nature*, 330, 244–246, doi:10.1038/330244a0.

Hair, J. E., R. E. Anderson, R. L. Tatham, and W. C. Black (1998), *Multivariate Data Analysis*, Prentice Hall, Upper Saddle River, N. J.

Harvey, J. W., J. E. Saiers, and J. T. Newlin (2005), Solute transport and storage mechanisms in wetlands of the Everglades, south Florida, *Water Resour. Res.*, 41, W05009, doi:10.1029/2004WR003507.

Harvey, J. W., R. W. Schaffranek, L. G. Larsen, D. Nowacki, G. B. Noe, and B. L. O'Connor (2008), Controls on flow velocity and flow resistance in the patterned floodplain landscape of the Everglades, paper presented at Ocean Sciences Meeting, Am. Soc. of Limnol. and Oceangr., Orlando, Fla., 2–7 March.

Hawley, N. (1982), Settling velocity distribution of natural aggregates, *J. Geophys. Res.*, 87, 9489–9498, doi:10.1029/JC087iC12p09489.

Hill, P. S., G. Voulgaris, and J. H. Trowbridge (2001), Controls on floc size in a continental shelf bottom boundary layer, *J. Geophys. Res.*, 106, 9543–9549, doi:10.1029/2000JC900102.

Kadlec, R. H. (1990), Overland flow in wetlands-vegetation resistance, *J. Hydraul. Eng.*, 116, 691–706, doi:10.1061/(ASCE)0733-9429(1990)116:5(691).

Khelifa, A., and P. S. Hill (2006), Models for effective density and settling velocity of flocs, *J. Hydraul. Res.*, 44, 390–401.

Krone, R. B. (1978), Aggregation of suspended particles in estuaries, in *Estuarine Transport Processes*, edited by B. Kjerfve, pp. 177–190, Univ. of S.C. Press, Columbia, S. C.

Larsen, L. G. (2008), Hydroecological feedback processes governing self-organization of the Everglades ridge and slough landscape, Univ. of Colo., Boulder.

Larsen, L. G., J. W. Harvey, and J. P. Crimaldi (2007), A delicate balance: Ecohydrological feedbacks governing landscape morphology in a lotic peatland, *Ecol. Monogr.*, 77, 591–614, doi:10.1890/06-1267.1.

Larsen, L. G., J. W. Harvey, G. B. Noe, and J. P. Crimaldi (2009), Predicting organic floc transport dynamics in shallow aquatic ecosystems: Insights from the field, the laboratory, and numerical modeling, *Water Resour. Res.*, 45, W01411, doi:10.1029/2008WR007221.

Li, D. H., and J. Ganczarczyk (1987), Stroboscopic determination of settling velocity, size and porosity of activated sludge flocs, *Water Res.*, 21, 257–262, doi:10.1016/0043-1354(87)90203-X.

Lick, W., J. Lick, and K. Ziegler (1992), Flocculation and its effect on the vertical transport of fine-grained sediments, *Hydrobiologia*, 235–236, 1–16, doi:10.1007/BF00026196.

Liss, S. N., I. G. Droppo, D. T. Flannigan, and G. G. Leppard (1996), Floc architecture in wastewater and natural riverine systems, *Environ. Sci. Technol.*, 30, 680–686, doi:10.1021/es950426r.

Logan, B. E., and D. B. Wilkinson (1990), Fractal geometry of marine snow and other biological aggregates, *Limnol. Oceanogr.*, 35, 130–136.

Manning, A. J., and K. R. Dyer (2002), The use of optics for the in situ determination of flocculated mud characteristics, *J. Opt. A Pure Appl. Opt.*, 4, S71–S81, doi:10.1088/1464-4258/4/4/366.

Mehta, A. J., and E. Partheniades (1975), An investigation of the depositional properties of flocculated fine sediments, *J. Hydraul. Res.*, 13, 361–381.

Meyer, J. L., and R. T. Edwards (1990), Ecosystem metabolism and turnover of organic carbon along a blackwater river continuum, *Ecology*, 71, 668–677, doi:10.2307/1940321.

Middleton, G. V., and P. R. Wilcock (1994), *Mechanics in the Earth and Environmental Sciences*, Cambridge Univ Press, Cambridge, U. K.

Mikkelsen, O. A., P. S. Hill, T. G. Milligan, and R. J. Chant (2005), In situ particle size distributions and volume concentrations from a LISST-100 laser particle sizer and a digital floc camera, *Cont. Shelf Res.*, 25, 1959–1978, doi:10.1016/j.csr.2005.07.001.

Milligan, T. G. (1996), In situ particle (floc) size measurements with the Benthos 373 plankton silhouette camera, *J. Sea Res.*, 36, 93–100, doi:10.1016/S1385-1101(96)90777-7.

National Research Council (2003), *Does Water Flow Influence Everglades Landscape Patterns?*, 41 pp., Natl. Acad., Washington, D. C.

Nepf, H. M. (1999), Drag, turbulence, and diffusion in flow through emergent vegetation, *Water Resour. Res.*, 35, 479–489, doi:10.1029/1998WR900069.

Nepf, H. M., and E. W. Koch (1999), Vertical secondary flows in submersed plant-like arrays, *Limnol. Oceanogr.*, 44, 1072–1080.

Newbold, J. D., S. A. Thomas, G. W. Minshall, C. E. Cushing, and T. Georgian (2005), Deposition, benthic residence, and resuspension

of fine organic particles in a mountain stream, *Limnol. Oceanogr.*, *50*, 1571–1580.

Nicholas, A. P., and D. E. Walling (1996), The significance of particle aggregation in the overbank deposition of suspended sediment on river floodplains, *J. Hydrol.*, *186*, 275–293, doi:10.1016/S0022-1694(96)03023-5.

Noe, G. B., L. J. Scinto, J. Taylor, D. L. Childers, and R. D. Jones (2003), Phosphorus cycling and partitioning in an oligotrophic Everglades wetland ecosystem: A radioisotope tracing study, *Freshwater Biol.*, *48*, 1993–2008, doi:10.1046/j.1365-2427.2003.01143.x.

Noe, G. B., J. Harvey, and J. Saiers (2007), Characterization of suspended particles in Everglades wetlands, *Limnol. Oceanogr.*, *52*, 1166–1178.

Nowell, A. R. M., P. A. Jumars, R. F. L. Self, and J. B. Southard (1989), The effects of sediment transport and deposition on infauna: Results obtained in a specially designed flume, in *Ecology of Marine Deposit Feeders*, edited by G. Lopez, G. Taghon, and J. Levinton, pp. 247–268, Springer, New York.

Ongley, E. D., B. G. Krishnappan, I. G. Droppo, S. S. Rao, and R. J. Maguire (1992), Cohesive sediment transport: Emerging issues for toxic chemical management, *Hydrobiologia*, *235–236*, 177–187, doi:10.1007/BF00026210.

Partheniades, E. (1977), Unified view of wash load and bed material load, *J. Hydraul. Div. Am. Soc. Civ. Eng.*, *103*, 1037–1057.

Pope, S. B. (2000), *Turbulent Flows*, Cambridge Univ. Press, Cambridge, U. K.

Ruddy, G., C. M. Turley, and T. E. R. Jones (1998), Ecological interaction and sediment transport on an intertidal mudflat II. An experimental dynamic model of the sediment-water interface, in *Sedimentary Processes in the Intertidal Zone*, edited by K. S. Black, D. M. Paterson, and A. Cramp, *Geol. Soc. Spec. Publ.*, vol. 139, pp. 149–166.

Shiono, K., C. F. Scott, and D. Kearney (2003), Predictions of solute transport in a compound channel using turbulence models, *J. Hydraul. Res.*, *41*, 247–258.

Simon, M., H. P. Grossart, B. Schweitzer, and H. Ploug (2002), Microbial ecology of organic aggregates in aquatic ecosystems, *Aquat. Microb. Ecol.*, *28*, 175–211, doi:10.3354/ame028175.

Sterling, M. C., Jr, J. S. Bonner, A. N. S. Ernest, C. A. Page, and R. L. Autenrieth (2005), Application of fractal flocculation and vertical transport model to aquatic soil-sediment systems, *Water Res.*, *39*, 1818–1830, doi:10.1016/j.watres.2005.02.007.

Stober, J., D. Scheidt, R. Jones, K. Thornton, L. Gandy, D. Stevens, J. Trexler, and S. Rathbun (1998), South Florida ecosystem assessment monitoring for adaptive management: Implications for ecosystem restoration, *Rep. EPA-904-R-98-002*, U.S. Environ. Prot. Agency, Washington, D. C.

Stone, M., and B. G. Krishnappan (2003), Floc morphology and size distributions of cohesive sediment in steady-state flow, *Water Res.*, *37*, 2739–2747, doi:10.1016/S0043-1354(03)00082-4.

Tambo, N., and Y. Watanabe (1979), Physical characteristics of flocs—1. The floc density function and aluminum floc, *Water Res.*, *13*, 409–419, doi:10.1016/0043-1354(79)90033-2.

Toorman, E. A. (2003), Validation of macroscopic modelling of particle-laden turbulent flows, paper presented at 6th Belgian National Congress on Theoretical and Applied Mechanics, Natl. Comm. on Theor. And Appl. Mech., Gent, Belgium.

Tsai, C. H., S. Iacobellis, and W. Lick (1987), Flocculation of fine-grained lake sediments due to a uniform shear stress, *J. Great Lakes Res.*, *13*, 135–146.

U.S. Army Corps of Engineers (1999), Central and southern Florida project, comprehensive review study, final integrated feasibility report and programmatic environmental impact statement, Washington, D. C.

Walling, D. E., and P. W. Moorehead (1989), The particle size characteristics of fluvial suspended sediment: An overview, *Hydrobiologia*, *176–177*, 125–149, doi:10.1007/BF00026549.

Ward, G. M., A. K. Ward, C. N. Dahm, and N. G. Aumen (1990), Origin and formation of organic and inorganic particles in aquatic systems, in *The Biology of Particles in Aquatic Systems*, edited by R. S. Wotton, pp. 27–56, CRC Press, Boca Raton, Fla.

Wetzel, R. G. (1995), Death, detritus, and energy flow in aquatic ecosystems, *Freshwater Biol.*, *33*, 83–89, doi:10.1111/j.1365-2427.1995.tb00388.x.

Wilcox, H. S., J. B. Wallace, J. L. Meyer, and J. P. Benstead (2005), Effects of labile carbon addition on a headwater stream food web, *Limnol. Oceanogr.*, *50*, 1300–1312.

Winterwerp, J. C., and W. G. M. van Kesteren (2004), *Introduction to the Physics of Cohesive Sediment in the Marine Environment*, Elsevier, Amsterdam.

Winterwerp, J. C., A. J. Bale, M. C. Christie, K. R. Dyer, S. Jones, D. G. Lintern, A. J. Manning, and W. Roberts (2002), Flocculation and settling velocity of fine sediment, in *Proceedings of the 6th International Conference on Nearshore and Estuarine Cohesive Sediment Transport, INTERCOH-2000*, *Proc. Mar. Sci.*, vol. 5, edited by J. C. Winterwerp and C. Kranenburg, pp. 25–40, Elsevier, Amsterdam.

Wolanski, E. (1995), Transport of sediment in mangrove swamps, *Hydrobiologia*, *295*, 31–42, doi:10.1007/BF00029108.

Wolanski, E., and R. J. Gibbs (1995), Flocculation of suspended sediment in the Fly River estuary, Papua New Guinea, *J. Coastal Res.*, *11*, 754–762.

Wotton, R. S. (2005), The essential role of exopolymers (EPS) in aquatic systems, *Oceanogr. Mar. Biol.*, *42*, 57–94.

Wotton, R. S. (2007), Do benthic biologists pay enough attention to aggregates formed in the water column of streams and rivers?, *J.N. Am. Benthol. Soc.*, *26*, 1–11, doi:10.1899/0887-3593(2007)26[1:DBBPEA]2.0.CO;2.

Wotton, R. S., and L. L. Warren (2007), Impacts of suspension feeders on the modification and transport of stream seston, *Arch. Hydrobiol.*, *169*, 231–236.

Zreik, D. A., B. G. Krishnappan, J. T. Germaine, O. S. Madsen, and C. C. Ladd (1998), Erosional and mechanical strengths of deposited cohesive sediments, *J. Hydraul. Eng.*, *124*, 1076–1085, doi:10.1061/(ASCE)0733-9429(1998)124:11(1076).

————————————————

P. Crimaldi, Department of Civil, Environmental, and Architectural Engineering, University of Colorado, 428 UCB, Boulder, CO 80309, USA.

J. W. Harvey and L. G. Larsen, U.S. Geological Survey, 430 National Center, Reston, VA 20192, USA. (lglarsen@usgs.gov)